
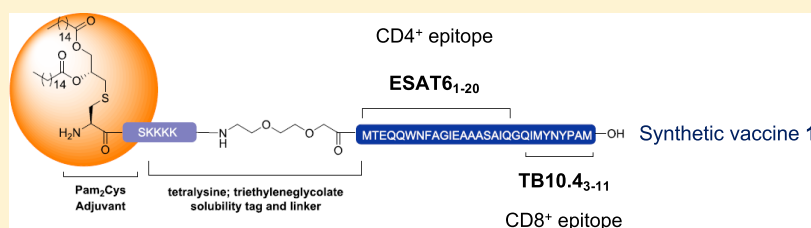


Mucosal Vaccination with a Self-Adjuvanted Lipopeptide Is Immunogenic and Protective against *Mycobacterium tuberculosis*

Anneliese S. Ashhurst,^{†,‡,||} David M. McDonald,^{†,||} Cameron C. Hanna,[†] Vicki A. Stanojevic,[†] Warwick J. Britton,^{*,‡,§} and Richard J. Payne^{*,†,§} 

[†]School of Chemistry, [‡]Tuberculosis Research Program Centenary Institute, and [§]Faculty of Medicine and Health, The University of Sydney, Camperdown, NSW 2050, Australia

Supporting Information



ABSTRACT: Tuberculosis (TB) remains a staggering burden on global public health. Novel preventative tools are desperately needed to reach the targets of the WHO post-2015 End-TB Strategy. Peptide or protein-based subunit vaccines offer potential as safe and effective generators of protection, and enhancement of local pulmonary immunity may be achieved by mucosal delivery. We describe the synthesis of a novel subunit vaccine via native chemical ligation. Two immunogenic epitopes, ESAT₆_{1–20} and TB10.4_{3–11} from *Mycobacterium tuberculosis* (Mtb), were covalently conjugated to the TLR2-ligand Pam₂Cys to generate a self-adjuvanting lipopeptide vaccine. When administered mucosally to mice, the vaccine enhanced pulmonary immunogenicity, inducing strong Th17 responses in the lungs and multifunctional peripheral T-lymphocytes. Mucosal, but not peripheral vaccination, provided substantial protection against Mtb infection, emphasizing the importance of delivery route for optimal efficacy.

INTRODUCTION

Tuberculosis (TB) has plagued human populations for a millennia and remains the leading cause of death from an infectious disease. The causative agent, *Mycobacterium tuberculosis* (Mtb), has the capacity to infect a healthy host and persist indefinitely without causing apparent disease, providing a reservoir of infection. Of the estimated 2 billion individuals colonized with Mtb, up to 10% will develop active disease in their lifetime.¹ In 2017, there were 1.6 million deaths and 10 million new cases of TB. Ten percent of these were children, indicating an ongoing active transmission.² The only available vaccine for TB, *Mycobacterium bovis* bacille Calmette–Guérin (BCG), is efficacious in reducing the risk of disseminated disease in infants, and its widespread use for TB protection is therefore likely to be continued into the future. However, BCG fails to prevent infection or provide long-term protection against the disease, and additionally is not considered suitable for use in immunocompromised individuals.³ There is therefore an urgent need to explore alternative approaches for the prevention of TB, including novel, safe, efficacious, and easily deliverable vaccines for use as boosters or BCG adjuncts. This is of particular importance considering the growing number of drug-resistant TB cases worldwide.^{4–6}

Recent clinical trials of peripheral vaccination with H4/IC31 or M72/AS01E, Mtb protein-based adjuvanted subunit vaccines that stimulate CD4⁺ T-lymphocyte responses,

demonstrated significant protection against new Mtb infection and pulmonary TB, respectively.^{7,8} Formulation of vaccines for pulmonary delivery has been explored for other infectious diseases^{9–11} and shows an opportunity to improve the immunogenicity and protective efficacy of TB vaccines by generating memory T lymphocytes in the lungs that may respond early to Mtb exposure.^{12,13} Pulmonary vaccination has additional practical advantages, as it negates the need for sterile needles, containment of sharps waste and large numbers of clinically trained personnel, lowering cost.¹² The viral-vectored vaccine, MVA85A, which failed to provide protection from TB in clinical studies when given as a peripheral vaccine,¹⁴ is now being examined as a pulmonary vaccine¹⁵ (Identifier: NCT01954563), with a supporting preclinical evidence that this route provides greater efficacy.¹⁶ Additionally, clinical trials are underway for an aerosol adenoviral-vectored TB vaccine (Ad85A; Identifier: NCT02337270) and aerosolized BCG (Identifier: NCT02709278). Safety concerns exist, however, regarding the use of live vaccines or viral vectors for pulmonary immunization, and repeat use may be limited due to immune responses to the viral backbone.^{17,18} Protein- or peptide-based subunit vaccines may provide a safer alternative, can be used in

Received: May 26, 2019

Published: August 2, 2019

65 immunocompromised individuals, and may be better suited for
66 repeat use.

67 While peptide-based vaccines successfully administer the
68 minimal amount of pathogenic material necessary to elicit an
69 immune response, they often suffer from poor immunoge-
70 nicity. Success in vivo is contingent upon co-administration of
71 immune-stimulating adjuvants. It has been shown by us and
72 others that covalent conjugation of adjuvants to peptide
73 vaccines is an effective means of achieving enhanced immune
74 responses compared to admixtures of individual components,
75 as this minimizes the separation of adjuvant and antigen in
76 vivo, potentiating immunogenicity.^{19–26} When considering
77 vaccines for pulmonary delivery, immune recognition receptors
78 should be selected that may be accessed at the pulmonary
79 mucosa and safely stimulated. Previous work in our laboratory
80 demonstrated the successful use of powdered pulmonary
81 vaccines, consisting of proteins from *Mtb* noncovalently
82 associated with a TLR2-ligand, as a safe and effective
83 immunization strategy for TB.²⁷ TLR2 agonists may be
84 particularly suitable for use in the pulmonary environment, as
85 the receptor is expressed on multiple cell types, including both
86 antigen-presenting cell subsets and pulmonary epithelial
87 cells.^{28–30} Of particular interest, a recent study demonstrated
88 the protective potential of lipopeptide combinations from the
89 *Mtb* protein antigen ESAT6 (Rv3875).³¹ We reasoned
90 therefore that covalent conjugation of peptide epitopes from
91 *Mtb* to a TLR2-ligand would lead to an effective self-
92 adjuvanted vaccine that may be more stable while providing
93 a robust immunological response.

94 ■ RESULTS AND DISCUSSION

95 Toward this end, we designed a self-adjuvanted vaccine
96 candidate **1** (Figure 1) based on the covalent conjugation of

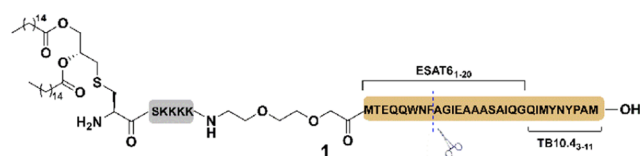
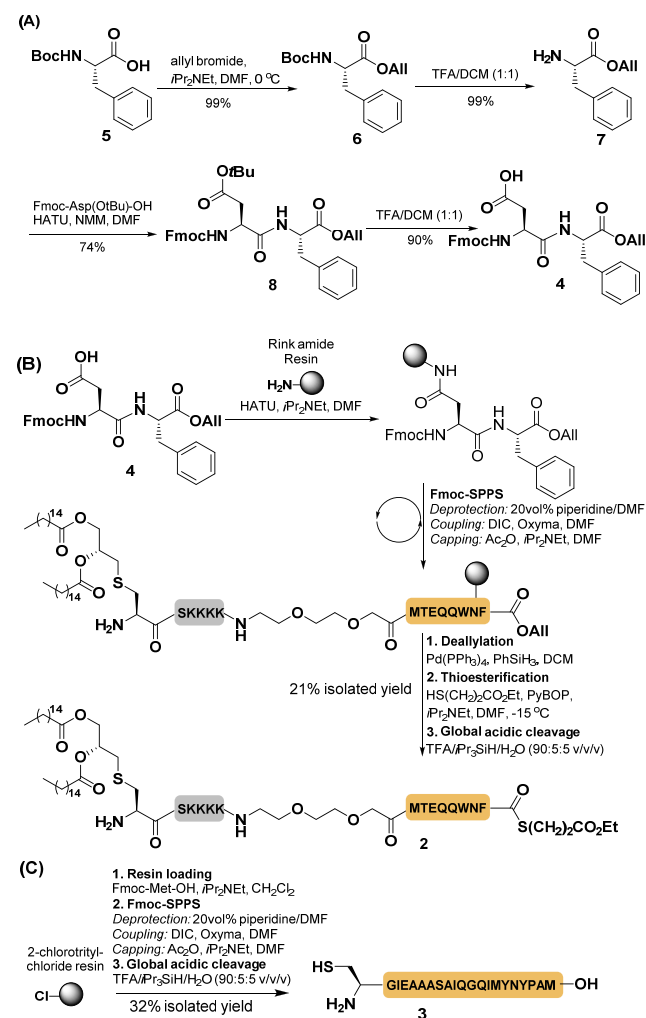


Figure 1. Self-adjuvanted vaccine candidate **1**, covalently conjugated Pam₂Cys as adjuvant and immunodominant T-lymphocyte epitopes from *Mtb*, ESAT6_{1–20} and TB10.4_{3–11}.

97 the TLR2/TLR6 agonist Pam₂Cys via a small flexible
98 triethylene glycol spacer to two antigenic peptides from the
99 *Mtb* proteins ESAT6 and TB10.4 (Rv0288 or ESX-H). These
100 peptides, ESAT6_{1–20} and TB10.4_{3–11}, possess immunodomi-
101 nant CD4⁺ and CD8⁺ T-lymphocyte epitopes, respectively, in
102 C57BL/6 mice. Initially, we attempted a linear synthesis of the
103 vaccine construct using Fmoc-strategy solid-phase peptide
104 synthesis (SPPS), but the lipophilicity of Pam₂Cys led to
105 difficulties in purifying the target vaccine to homogeneity. We
106 therefore turned to a native chemical ligation strategy for the
107 convergent and chemoselective fusion of peptide fragments to
108 generate larger constructs.³² It was envisaged that a native
109 chemical ligation strategy would permit initial synthesis of a
110 shorter and easily purifiable lipopeptide thioester fragment,
111 which could then be rapidly conjugated to the rest of the
112 vaccine construct. To reduce the number of purification steps,
113 2,2,2-trifluoroethanethiol (TFET) was selected as a thiol
114 additive to promote rapid ligation while enabling in situ radical
115 desulfurization to access the target vaccine **1** (with a native

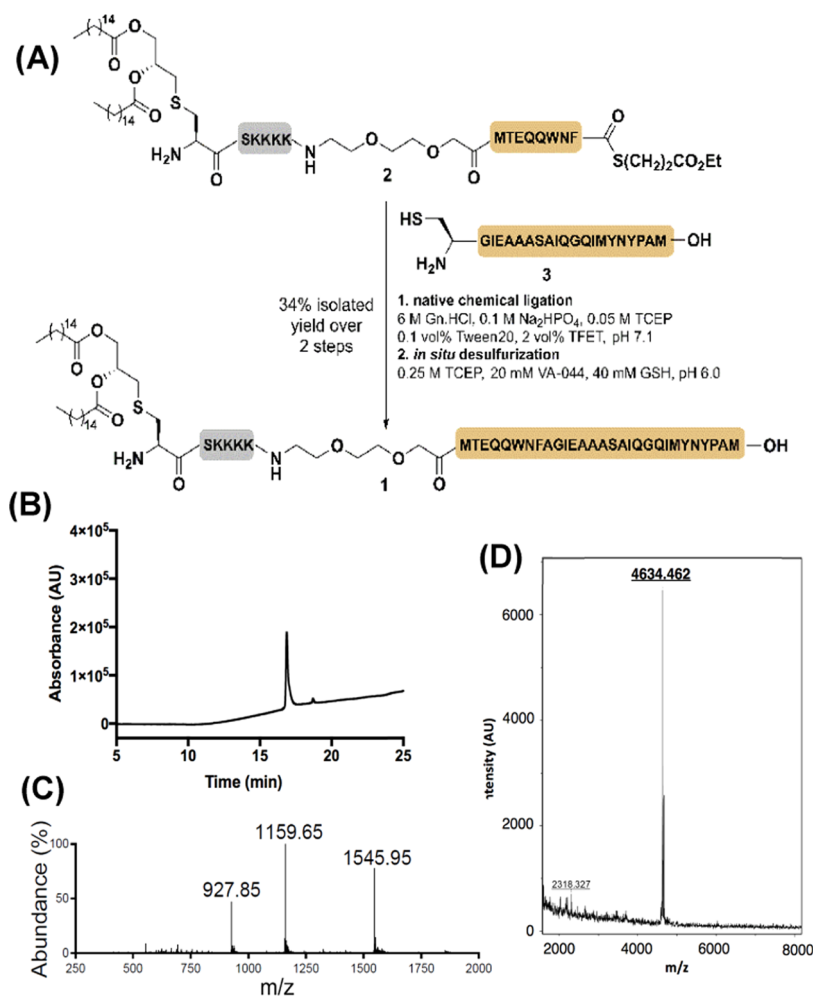
alanine residue at ligation junction) in a one-pot manner.³³
With this synthetic strategy in mind, we chose to disconnect
the vaccine between Phe8 and Ala9 of the ESAT6 epitope
(Figure 1). This led to two synthetic targets, lipopeptide
thioester **2**, bearing an N-terminal Pam₂Cys residue (Scheme
1B), and peptide **3**, possessing an N-terminal cysteine in place
of native Ala9 in the ESAT6 epitope (Scheme **1C**).

Scheme 1. (A) Synthesis of Dipeptide Building Block **4** from Boc-Phe-OH; (B) Synthesis of Lipopeptide Thioester Fragment **2** via Side Chain Anchoring, Fmoc-SPPS and Subsequent On-Resin Thioesterification; NB: Amino Acids within Resin-Bound Peptides Possess Standard Side-Chain-Protecting Groups Used in Fmoc-SPPS; (C) Synthesis of Peptide Fragment **3** via Fmoc-SPPS



Synthesis of lipopeptide thioester **2** was achieved via Fmoc-
strategy SPPS on Rink amide resin using an on-resin
thioesterification procedure.³⁴ Initially, we synthesized Fmoc-
AspPhe-OAll **4** (Scheme **1A**). This began by allyl ester
protection of Boc-Phe-OH (**5**) to afford **6**, followed by Boc
deprotection and coupling to Fmoc-Asp(OtBu)-OH to afford
dipeptide **8** in good yield. Deprotection of the side-chain tBu
ester on the aspartate residue then provided the target
dipeptide **4**. With **4** in hand, it was next loaded via the
condensation of the side-chain carboxylate of the aspartate
residue to Rink amide resin (Scheme **1B**). The polypeptide
chain was then elongated using iterative Fmoc-SPPS, with **134**

Scheme 2. (A) Synthesis of Self-Adjuvanting Tuberculosis Vaccine Candidate **1** via One-Pot Native Chemical Ligation and Desulfurization; (B) Analytical HPLC Chromatogram, (C) electrospray ionization mass spectrometry (ESI-MS), and (D) matrix-assisted laser desorption/ionization time-of-flight (MALDI-TOF) MS Spectrum of Vaccine **1**



135 amino acid, triethyleneglycolate, and Pam₂Cys couplings
 136 effected with *N,N'*-diisopropylcarbodiimide (DIC) and ethyl
 137 (hydroxyimino)cynoacetate (Oxyma). At this point, the allyl
 138 ester-protected C-terminus of the peptide was unmasked by
 139 treatment with palladium *tetrakis*-triphenylphosphine and
 140 phenylsilane. Treatment with ethyl 3-mercaptopropionate in
 141 the presence of (benzotriazole-1-yl)oxy-
 142 tripyrrolidinophosphonium hexafluorophosphate (PyBOP)
 143 and *N,N*-diisopropylethylamine at -15 °C^{35,36} led to the
 144 formation of the C-terminal thioester with no detectable
 145 epimerization. Cleavage of the peptide thioester using an acidic
 146 cocktail comprising trifluoroacetic acid (TFA), triisopropylsi-
 147 lane, and water provided the crude lipopeptide thioester, which
 148 was purified via reverse-phase high-performance liquid
 149 chromatography (HPLC) to afford **2** in 21% yield (over 43
 150 steps calculated from the initial resin loading). Peptide **3** was
 151 also accessed via Fmoc-strategy SPPS and isolated in 32% yield
 152 (over 63 iterative steps based on the initial resin loading)
 153 following reverse-phase HPLC (on C18 stationary phase)
 154 (Scheme 1C).

155 With the two target fragments in hand, our attention turned
 156 to the key ligation–desulfurization assembly of vaccine **1**.
 157 Native chemical ligation is typically carried out in aqueous
 158 phosphate buffer (0.1 M, pH ~7) containing tris-

(carboxyethyl)phosphine (TCEP, 50 mM) as a reductant 159
 and guanidine hydrochloride (Gdn.HCl, 6 M) as a denaturing 160
 agent. However, lipopeptide thioester **2** was insoluble in this 161
 buffer system and, as a result, we supplemented the buffer with 162
 the nonionic surfactant Tween-20 (0.5% v/v) as a solubilizing 163
 detergent. Specifically, lipopeptide thioester **2** and peptide **3** 164
 were dissolved in this buffer and 2,2,2-trifluoroethanethiol 165
 (TFET, 2% v/v) was added.³³ Pleasingly, within 2 h, the 166
 reaction proceeded to completion to afford the ligation 167
 product. Without purification, *in situ* desulfurization of the 168
 ligation product was performed through treatment with the 169
 radical initiator 2,2'-azobis[2-(2-imidazolin-2-yl)propane]- 170
 dihydrochloride (VA-044) (20 mM) in the presence of 171
 reduced glutathione (40 mM) and TCEP (250 mM) to 172
 convert the cysteine to a native alanine residue at the ligation 173
 junction. HPLC purification using C18 reverse-phase HPLC 174
 furnished self-adjuvanting TB vaccine candidate **1** in 34% yield 175
 over two steps (Scheme 2). 176 s2

The adjuvant activity of the synthesized conjugate vaccine **1** 177
 was first verified *in vitro*. Specifically, Pam₂Cys binding and 178
 activation of the TLR2 signaling pathway was assessed in a 179
 HEK-TLR2-reporter cell line. Conjugate vaccine **1** showed a 180
 strong activation of TLR2, comparable to stimulation with 181
 Pam₂Cys-SKKKK-PEG(OH) (Figure 2). The *in vivo* 182 s2

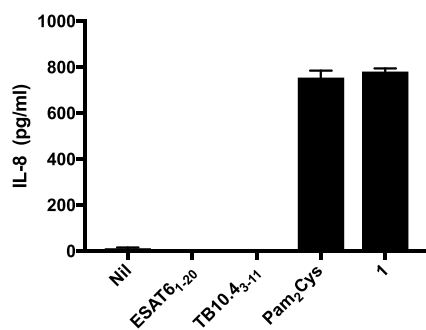


Figure 2. Vaccine candidate **1** activates TLR2 signaling in vitro. Stimulation of IL-8 released from HEK-TLR2 reporter cells by synthetic conjugate **1** is shown in comparison to stimulation with PBS (Nil), ESAT6_{1–20} or TB10.4_{3–11} peptides, or Pam₂Cys-PEG(OH) alone (at ~7 μM). Data are mean ± standard error of the mean (SEM) (*n* = 3) and are representative of two independent experiments.

183 immunogenicity induced by **1** was assessed in mice; three
184 homologous vaccinations were given 2 weeks apart and
185 responses were assessed 3 weeks after the final vaccination.
186 Mice were immunized at either the pulmonary mucosa via
187 intranasal (i.n.) instillation or peripherally by subcutaneous
188 (s.c.) injection. The use of defined immunodominant peptide
189 epitopes as antigens enabled quantitative and qualitative
190 assessment of the CD4⁺ and CD8⁺ T-lymphocyte responses
191 generated both locally and systemically. Lymphocytes from the
192 lungs and spleens of immunized mice were restimulated with
193 ESAT6_{1–20} or TB10.4_{3–11} peptides ex vivo prior to intracellular
194 immunostaining and flow cytometry. Mucosal delivery of **1**

induced substantial populations of ESAT6-specific CD4⁺ T-
lymphocytes in the lungs producing IL-17 and TNFα (Figure
3A). The multifunctionality of local T-lymphocytes were also
increased, such that significant populations of IL-17⁺ CD4⁺
cells were observed that also expressed other key cytokines,
including IFNγ, IL-2, and TNFα, indicative of a predominantly
Th17-like phenotype (Figure S1). Notably, there was minimal
detectable cytokine response in the lungs of mice that were
vaccinated s.c. (Figures 3A and S1). The profile of cytokine-
producing ESAT6-specific CD4⁺ T-lymphocytes in the spleens
of mucosally immunized mice was similar to that seen in the
lungs, but additionally with enhanced IL-2 responses (Figures
3B and S2). A minor population of IL-2- and TNFα-producing
cells were observed in the spleens of s.c. immunized mice;
however, no other significant populations were identified
(Figures 3B and S2). No significant cytokine-producing CD8⁺
populations were seen in the lungs of any immunized group in
response to TB10.4_{3–11} (Figure S3A), but small populations of
IFNγ- and TNFα-producing CD8⁺ cells were seen in the
spleens of s.c. immunized mice (Figure S3B). This may
indicate that murine leukocytes were not able to efficiently
process this epitope from **1** appropriately for presentation to
CD8⁺ T-lymphocytes. Overall, mucosal delivery of the vaccine
candidate **1** substantially improved pulmonary immunogenicity
and preferentially led to a strong Th17-like CD4⁺ T-
lymphocyte response.

Adjuvants for new vaccines should ideally be selected based
on their ability to induce the type of immune response best
correlated with protection against the pathogen. In the case of
Mtb, there is strong evidence that a Th1-type CD4⁺ T-
lymphocyte response is required; however, this is not sufficient

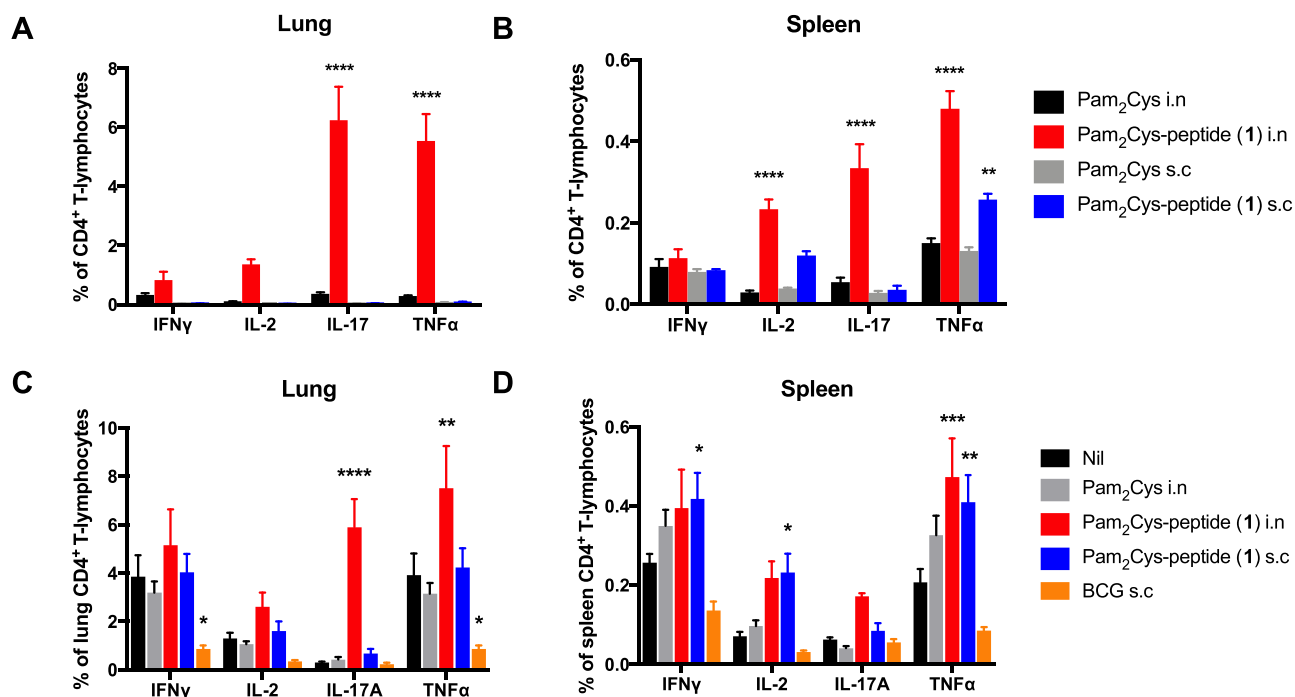


Figure 3. Mucosal, but not peripheral, delivery of **1** induces a strong antigen-specific pulmonary IL-17 and TNFα responses that are maintained post-Mtb challenge. Frequency of cytokine-producing CD4⁺ T-lymphocytes in the (A) lungs and (B) spleen 3 weeks following final immunization (*n* = 3) and (C) lungs and (D) spleen 4 weeks post-Mtb challenge (*n* = 6). Epitope-specific cells were detected by intracellular immunostaining and flow cytometry after recall with ESAT6_{1–20} (10 μg/mL). Data are mean ± SEM. Statistically significant differences (A, B) to relevant Pam₂Cys control by analysis of variance (ANOVA) with Tukey's multiple comparison test, and (C, D) to Nil control, by ANOVA with Dunnett's multiple comparison test (**p* < 0.05, ***p* < 0.01, ****p* < 0.001, *****p* < 0.0001).

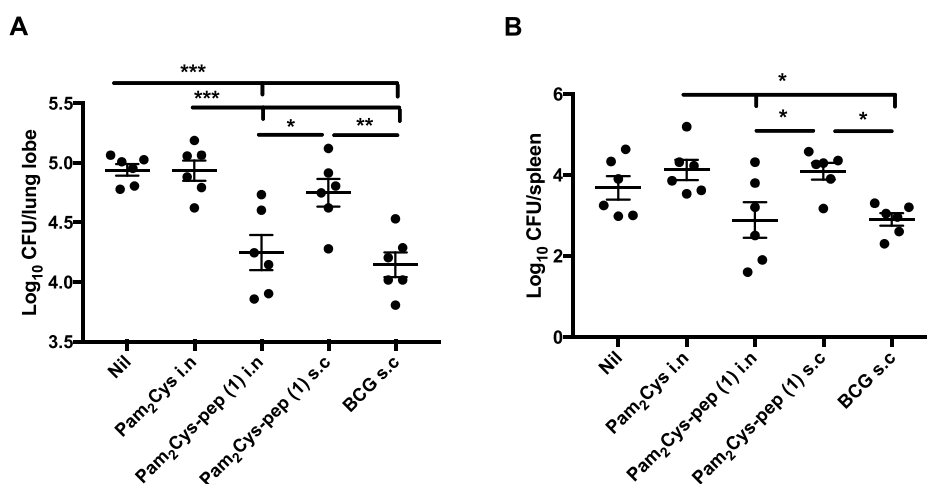


Figure 4. Protective efficacy against Mtb infection was induced by mucosal immunization with **1**. Mice ($n = 6$) were immunized with **1** ($10 \mu\text{g}$ peptide component), or an equivalent amount of Pam₂Cys, three times at two-weekly intervals. Six weeks later, the mice were challenged with aerosol Mtb H37Rv (100 CFU). Alternatively, the mice received $5 \times 10^5 \text{ CFU}$ BCG s.c. 10 weeks before challenge. After 28 days, the bacterial loads in (A) lungs and (B) spleen were enumerated. Data are mean \pm SEM and are representative of two independent experiments. Statistical significance was determined by ANOVA with Tukey's multiple comparisons test (* $p < 0.05$, ** $p < 0.01$, *** $p < 0.001$).

226 for sterilizing immunity.³⁷ Immunization at the pulmonary
 227 mucosa tends to drive a Th17-based response to peptide
 228 antigens, likely due to the induction of IL-1, IL-6, and TGF β
 229 expression.^{38,39} TLR2 stimulation, which leads to the
 230 production of TNF and IL-6, is critical for the activation of
 231 antigen-presenting cells²⁸ and are also inducers of Th17
 232 polarization, characterized by IL-17, IL-21, and IL-22
 233 production. IL-17 may promote granuloma formation and
 234 neutrophil recruitment by inducing the pro-inflammatory
 235 cytokines and chemokines G-CSF, IL-6, and IL-8,^{40,41} as well
 236 as recruitment of IFN γ -producing cells to the site of infection
 237 by induction of CXCL10 expression.⁴² This is suggested to be
 238 one of the mechanisms by which Th17 cells may promote the
 239 immune response to Mtb.⁴³ While the role of vaccine-induced
 240 IL-17 in protection against Mtb is controversial,^{44,45} several
 241 studies have indicated the plasticity of vaccine-induced Th17
 242 cells in mice, and their capacity to revert after exposure to Mtb
 243 to expression of the classical Th1-associated cytokine IFN γ ,
 244 even after long-term residency as memory cells in the
 245 lungs.^{46,47} It is therefore possible that mucosal immunization
 246 with **1**, despite inducing primarily strong Th17 responses, may
 247 provide a pool of lung resident CD4⁺ T-lymphocytes that can
 248 function as Th1 or Th17 as needed and provide protective
 249 responses against the pathogen.^{12,13}

250 Having demonstrated robust pulmonary immunogenicity
 251 from mucosal administration of **1**, we next tested the self-
 252 adjuvanting vaccine candidate in an aerosol Mtb infection.
 253 C57BL/6 mice received three homologous immunizations 3
 254 weeks apart with i.n. Pam₂Cys alone or **1** by i.n. instillation or
 255 s.c. injection. A separate group of mice received BCG s.c.,
 256 considered the gold-standard comparison in murine models of
 257 Mtb challenge.⁴⁸ After 6 weeks, the mice were challenged by
 258 aerosol with Mtb and the postchallenge immune response to
 259 the vaccine epitopes were assessed 4 weeks later. Mice
 260 immunized i.n. with **1** had maintained significantly upregulated
 261 populations of ESAT6-specific CD4⁺ T-lymphocytes produc-
 262 ing IL-17 and TNF α in the lungs, which were not seen in
 263 peripherally immunized mice (Figure 3C). The diversity of
 264 multifunctional cytokine-producing populations in the lungs of
 265 mucosally immunized mice was maintained postchallenge

(Figure S4). Populations of a similar phenotype were also seen
 266 in the spleen (Figures 3D and S5), consistent with the
 267 immunogenicity pre-Mtb challenge. At this postchallenge
 268 stage, mice immunized s.c. had increased ESAT6-specific
 269 IFN γ ⁺, IL-2⁺, and TNF α ⁺ CD4⁺ T-lymphocyte populations in
 270 the spleen (Figures 3D and S5). There were minimal vaccine-
 271 induced responses seen to the TB10.4₃₋₁₁ peptide post-
 272 challenge, and it is likely that these populations reflect
 273 responses to the Mtb challenge itself (Figure S6).
 274

To assess if the T-lymphocyte responses generated by **1**
 275 were functionally beneficial, the Mtb bacterial burden in the
 276 lungs and spleen were enumerated to determine the protective
 277 efficacy of the vaccine. We were pleased to observe that when **1**
 278 was delivered mucosally, it provided substantial protection in
 279 both the lungs and spleen, similar to that provided by BCG
 280 (Figure 4). Consistent with the immunological data, while
 281 there was a trend toward protection in the lungs after
 282 subcutaneous vaccination, this did not reach statistical
 283 significance in all experiments (Figure 4A) and no protection
 284 was seen in the spleen (Figure 4B). These data strongly
 285 support the model that vaccination strategies promoting a
 286 pulmonary immune response offer more robust protection
 287 from Mtb. Taken together, this study provides an exciting
 288 proof of principle data that synthetic self-adjuvanting peptide
 289 vaccines can provide substantial pulmonary immunogenicity
 290 and protection against virulent Mtb.
 291

292 ■ CONCLUSIONS

In summary, we have successfully produced a synthetic
 293 lipopeptide conjugate vaccine candidate **1** by one-pot native
 294 chemical ligation–desulfurization chemistry and assessed the
 295 delivery by pulmonary or peripheral routes to induce
 296 protective immune responses to Mtb. Mucosal delivery offered
 297 increased immunogenicity and protective efficacy. The use of
 298 this vaccine in humans will depend on future toxicology and
 299 careful evaluation of the adjuvant Pam₂Cys in phase I clinical
 300 studies. It will be important in future studies to assess whether
 301 pulmonary vaccination with constructs such as **1** may be used
 302 to boost the protective efficacy of BCG or improve the long-
 303 term protective efficacy against Mtb. Pulmonary boosting may
 304

305 have the additional benefit of drawing memory T-lymphocytes
306 generated by subcutaneous BCG into the lungs, creating a
307 further reservoir of memory cells that may act quickly to
308 combat future encounter with Mtb. Further, these conjugated
309 lipopeptides provide the means to assess the impact that the
310 type of conjugation between antigen and adjuvant has on
311 immunogenicity and protective efficacy. The ligation technol-
312 ogy employed in this study is applicable to the conjugation of
313 diverse peptide or protein antigens to different adjuvants that
314 stimulate a variety of pattern recognition receptors. Exploring
315 pulmonary administration to enhance efficacy and ease of
316 delivery with a range of different adjuvants and antigens from
317 Mtb may contribute novel constructs to the TB vaccine
318 pipeline and will be the subject of continued work in our
319 laboratories.

320 ■ EXPERIMENTAL SECTION

321 **General Methods.** Unless otherwise stated, reactions were carried
322 out under an argon atmosphere and at room temperature (rt) (22
323 °C). Reactions carried out at 0 °C employed a bath of water and ice.
324 Anhydrous CH₂Cl₂ and dimethylformamide (DMF) was obtained
325 using a PureSolv solvent purification system (water < 10 ppm).
326 Reactions were monitored by thin layer chromatography (TLC) on
327 aluminum-backed silica plates (Merck Silica Gel 60 F254). Visual-
328 ization of TLC plates was undertaken with an ultraviolet light at λ =
329 254 nm and staining with solutions of vanillin or phosphomolybdic
330 acid, followed by exposure of the stained plates to heat. Silica gel 60
331 40–63 μm was used for flash column chromatography. NMR
332 spectroscopy was performed in CDCl₃ on a Bruker DRX 300 or
333 DRX 400 NMR spectrometer at frequencies of 300 MHz or 400 MHz
334 for ¹H NMR and 75 or 100 MHz for ¹³C NMR, respectively.
335 Chemical shifts are reported in parts per million (ppm) and coupling
336 constants in Hertz (Hz). Residual solvent was used as internal
337 standards (CDCl₃: δ_H = 7.26, δ_C = 77.16). ¹³C NMR data are
338 reported as chemical shift values (ppm). Mass spectrometry with
339 electrospray ionization (ESI) was performed on a Shimadzu 2020
340 (ESI) mass spectrometer operating in a positive mode. High-
341 resolution mass spectra were recorded on a Bruker-Daltonics Apex
342 Ultra 7.0T Fourier transform (FTICR) mass spectrometer. MALDI-
343 TOF mass spectrometry was performed on a Bruker Autoflex Speed
344 MALDI-TOF mass spectrometer operating in reflectron mode using a
345 matrix of 10 mg/mL α-cyano-4-hydroxycinnamic acid in water/
346 acetonitrile containing 0.1% TFA (1:1 v/v). Optical rotations were
347 measured on a PerkinElmer 341 polarimeter at a wavelength of 589
348 nm. IR spectra were recorded on a Bruker Alpha FT-IR spectrometer
349 using a diamond ATR unit. The purity of all compounds was >97% as
350 judged by NMR spectroscopy and HPLC.

351 **General Procedure for Fmoc-SPPS.** Fmoc-SPPS was performed
352 on a Biotage Initiator+ Alstra microwave peptide synthesizer using the
353 following conditions. Amino acid coupling: A solution of Fmoc-
354 protected amino acid (4 equiv), DIC (4 equiv), and Oxyma (4 equiv)
355 in DMF (Labskan, final amino acid concentration 0.1 M) was added
356 to the resin. After 30 min at 50 °C, the resin was washed with DMF
357 (5 × 5 mL). Deprotection: The resin was treated with 20%
358 piperidine/DMF (2 × 3 mL, 3 min) at rt and then washed with
359 DMF (5 × 5 mL). Capping: Ac₂O/pyridine (1:9 v/v) was added to
360 the resin (3 mL). After 3 min, the resin was washed with DMF (5 × 5
361 mL).

362 **General Procedure for Resin Cleavage.** Peptides were cleaved
363 from resin (with concomitant side-chain deprotection) by treatment
364 with an acidic cocktail containing TFA/triisopropylsilane/water
365 (90:5:5 v/v/v) with gentle shaking for 2 h. The cleavage solution
366 was filtered and the resin washed with TFA (2 × 2 mL). The solution
367 was concentrated and then precipitated with cold diethyl ether. The
368 mixture was centrifuged and the supernatant was discarded.

369 **Preparative and Semipreparative Reverse-Phase HPLC.**
370 HPLC purification was performed using a Waters 600 Multisolvant
371 Delivery System and Waters 500 pump with a Waters 490E

programmable wavelength detector operating at 214, 230, or 280
372 nm. Peptide 3 was purified by preparative HPLC on a Waters Sunfire
373 C18 column (5 μm, 19 × 150 mm) at a flow rate of 7 mL min⁻¹
374 (solvent A: 0.1% TFA in H₂O; solvent B: 0.1% TFA in MeCN).
375 Lipopeptides 1 and 2 were purified by semipreparative HPLC on a
376 Phenomenex Luna C18(2) column (5 μm, 10 × 250 mm) in a
377 column heater at 40 °C and a flow rate of 7 mL min⁻¹ (solvent A:
378 0.1% TFA in H₂O:MeCN:iPrOH (8:1:1 v/v/v); solvent B: 0.1% TFA
379 in MeCN:iPrOH (9:1 v/v)).
380

381 **Synthesis of Vaccine 1 via One-Pot Native Chemical**
382 **Ligation Desulfurization.** Lipopeptide thioester 2 (2.5 mg, 0.96
383 μmol) and peptide 3 (2 equiv, 4.2 mg, 1.92 μmol) were dissolved in
384 aqueous phosphate buffer (0.1 M, pH = 7.4, 192 μL, 5 mM with
385 respect to thioester 2) containing guanidine hydrochloride (6 M),
386 TCEP (50 mM), and Tween-20 (0.5% v/v). The pH of the reaction
387 mixture was adjusted with aqueous NaOH (1 M) to pH 7.2. TFET
388 (2% v/v) was added and the reaction was incubated at 37 °C for 2 h.
389 The reaction was followed by ultraperformance liquid chromatog-
390 raphy-tandem mass spectrometry (UPLC-MS). After consumption of
391 the thioester (as measured by UPLC-MS analysis, 2 h) the reaction
392 was degassed under a stream of argon, and one volume of degassed
393 aqueous phosphate buffer containing guanidine hydrochloride (6 M),
394 TCEP (500 mM), reduced glutathione (80 mM), and the radical
395 initiator VA-044 (40 mM) was added. The reaction was allowed to
396 proceed at 37 °C for 8 h, at which time the ligation product bearing
397 cysteine at the ligation junction was fully converted to the
398 corresponding alanine-containing product (as judged by UPLC-MS
399 analysis). Semipreparative HPLC purification (0–60% B over 40 min,
400 7 mL min⁻¹, 40 °C, Phenomenex Luna C18(2), 5 μm, 100 Å, 10 ×
401 250 mm) followed by lyophilization afforded pure vaccine candidate 1
402 as a white solid (1.5 mg, 34% yield). Analytical HPLC: R_t 16.9 min
403 symmetry C4 column, 300 Å, 5 μm, 4.6 mm × 250 mm, gradient:
404 20–100 B over 25 min (solvent A: H₂O + 0.1% TFA, solvent B:
405 MeCN + 0.1% TFA); MS calcd: [M + 3H]³⁺ = 1545.48, [M + 4H]⁴⁺
406 = 1159.36, [M + 5H]⁵⁺ = 927.69; found (ESI⁺): 1545.95, 1159.65,
407 927.85. HRMS calcd for C₂₁₄H₃₄₈N₄₇O₅₈S₄: [M + H]⁺ = 4634.466;
408 found (MALDI-TOF): 4634.462.

409 **Synthesis of Lipopeptide Thioester 2.** Rink amide resin (25
410 μmol, 0.3 mmol/g loading) was initially washed with CH₂Cl₂ (5 × 3
411 mL) and DMF (5 × 3 mL), followed by Fmoc deprotection with 20%
412 piperidine/DMF (2 × 5 min). The resin was washed with DMF (5 ×
413 3 mL), CH₂Cl₂ (5 × 3 mL), and DMF (5 × 3 mL). PyBOP (4 equiv)
414 and N-methylmorpholine (NMM) (8 equiv) were added to a solution
415 of Fmoc-AspPhe-OAll 4 (4 equiv) in DMF. After 5 min of
416 preactivation, the mixture was added to the resin and then shaken
417 at rt for 2 h. The resin was filtered, then washed with DMF (5 × 3
418 mL), CH₂Cl₂ (5 × 3 mL), and DMF (5 × 3 mL), capped with Ac₂O/
419 pyridine (1:9 v/v; 2 × 3 min), and washed with DMF (5 × 3 mL),
420 CH₂Cl₂ (5 × 3 mL), and DMF (5 × 3 mL). The resin-bound H-
421 SKKKK-triethyleneglycolate-ESAT6(1–8) peptide was synthesized
422 on the side-chain-loaded resin using the general procedure for Fmoc-
423 SPPS. For the coupling of Pam₂Cys, a solution of Fmoc-Pam₂Cys-OH
424 (1.2 equiv), DIC (1.2 equiv), and HOAt (1.5 equiv) in DMF was
425 added to the resin, and the reaction was shaken at rt for 16 h. The
426 resin was next treated with a solution of Pd(PPh₃)₄ (1 equiv) and
427 PhSiH₃ (40 equiv) in dry CH₂Cl₂. The resin was shaken for 1 h and
428 the procedure was repeated. Afterward, the resin was washed with
429 CH₂Cl₂ (10 × 5 mL), DMF (5 × 5 mL), and CH₂Cl₂ (5 × 5 mL). A
430 solution of ethyl-3-mercaptopropionate (4 equiv) and PyBOP (4
431 equiv) in DMF (2–3 mL) was added to the resin at –15 °C in a salt-
432 ice–water bath. Subsequently, ¹Pr₂NEt (4 equiv) was added to the
433 resin. The resin was left at –15 °C for 3 h. Afterward, the resin was
434 washed with CH₂Cl₂ (10 × 5 mL), DMF (5 × 5 mL), and CH₂Cl₂ (5
435 × 5 mL). The peptide was cleaved from resin and worked up as
436 described in the general resin cleavage procedure. The dried pellet
437 was dissolved in water containing 40% MeCN + 0.1% TFA, purified
438 by preparative RP-HPLC (50–100% B over 40 min, 4 mL min⁻¹, 40
439 °C, Phenomenex Luna C18(2), 5 μm, 100 Å, 10 × 250 mm) and
440 lyophilized to afford the desired lipopeptide thioester as a white solid
441 (13.5 mg, 21% yield). Analytical HPLC: R_t 16.0 min (50–100% B

442 over 30 min, 0.2 mL min⁻¹, Phenomenex Luna C18(2), 5 μm, 2.1 ×
443 150 mm, λ = 214 nm). MS calcd: [M + 2H]²⁺ = 1300.24, [M + 3H]³⁺
444 = 867.17, [M + 4H]⁴⁺ = 650.62; found (ESI⁺): 1300.80, 867.45,
445 650.75.

446 **Synthesis of Peptide 3.** 2-Chlorotrityl chloride resin (50 μmol,
447 1.22 mmol/g loading) was swollen in dry CH₂Cl₂ for 30 min then
448 washed with CH₂Cl₂ (5 × 3 mL). A solution of Fmoc-Met-OH (0.5
449 equiv relative to resin functionalization) and ⁱPr₂NEt (2.0 equiv
450 relative to resin functionalization) in CH₂Cl₂ (final amino acid
451 concentration 0.1 M of amino acid) was added and the resin was
452 shaken at rt for 16 h. The resin was washed with DMF (5 × 3 mL)
453 and CH₂Cl₂ (5 × 3 mL). The resin was treated with a solution of
454 CH₂Cl₂/CH₃OH/ⁱPr₂NEt (17:2:1 v/v/v, 3 mL) for 1 h and washed
455 with DMF (5 × 3 mL), CH₂Cl₂ (5 × 3 mL), and DMF (5 × 3 mL).
456 The ESAT6(9–20)-TB10.4(3–11) peptide was synthesized via
457 Fmoc-strategy solid-phase peptide synthesis as outlined in the general
458 methods section. The peptide was cleaved from resin and worked up
459 via the general resin cleavage procedure. The dried pellet was
460 dissolved in water containing 30% MeCN + 0.1% TFA and purified by
461 preparative HPLC (0–60% B over 40 min, 7 mL min⁻¹, Sunfire C18,
462 5 μm, 100 Å, 19 × 150 mm) to afford the desired peptide as a white
463 solid (35 mg, 32% yield). Analytical HPLC: R_t 13.1 min (0–100% B
464 over 30 min, 0.2 mL min⁻¹, 0.1% TFA, Sunfire C18, 5 μm, 100 Å, 2.1
465 × 150 mm, λ = 214 nm). MS calcd: [M + 2H]²⁺ = 1102.50, [M +
466 3H]³⁺ = 735.33; found (ESI⁺): 1102.60, 734.45.

467 **Fmoc-L-Asp-L-Phe-OAll (4).** The protected dipeptide **8** (872 mg,
468 1.42 mmol) was treated with TFA in CH₂Cl₂ (10 mL, 1:1 v/v). The
469 reaction mixture was stirred at room temperature for 1 h, after which
470 the TFA/CH₂Cl₂ solvent mixture was removed under a gentle stream
471 of nitrogen. The residue was dissolved in CH₂Cl₂ and then washed
472 with water (2 × 30 mL), saturated aqueous NaHCO₃ solution (2 ×
473 30 mL), and brine (30 mL). The organic phase was dried with
474 anhydrous MgSO₄, concentrated in vacuo, and purified by flash
475 column chromatography to afford the target compound **4** as a yellow
476 oil (728 mg, 90% yield). R_f = 0.42 (EtOAc/hexane: 1:2 v/v) ¹H NMR
477 (CDCl₃, 400 MHz) δ (ppm): 7.77 (d, J = 7.41 Hz, 2H), 7.54 (m,
478 2H), 7.39 (t, J = 7.4 Hz, 2H), 7.29 (t, J = 7.4 Hz, 2H), 7.20–7.08 (m,
479 6H), 5.97 (d, 8.1 Hz, 1H), 5.82 (ddt, J = 5.5, 10.5, 16.5 Hz, 1H), 5.25
480 (dd, J = 17.9, 10.5 Hz, 2H), 4.85 (dd, 6.3, 6.8 Hz, 1H), 4.56 (m, 3H),
481 4.42–4.34 (m, 2H), 4.18 (t, J = 7.0 Hz, 1H), 3.12–3.06 (m, 3H),
482 2.70 (m, 1H); ¹³C NMR (CDCl₃, 100 MHz) δ (ppm): 170.8, 156.1,
483 143.6, 141.3, 141.2, 135.5, 131.2, 129.2, 128.5, 128.5, 127.8, 127.2,
484 127.1, 125.1, 120.0, 119.1, 67.5, 66.2, 53.6, 50.7, 47.0, 37.7, 35.9;
485 HRMS: (+ESI) Calc. for 542.2053 [M + Na]⁺, found: 542.2058 [M +
486 Na]⁺; IR (ATR): ν_{max} = 3300, 3065, 3030, 2924, 2854, 1710, 1661,
487 1532, 1449, 1248, 1211, 1049, 738, 701 cm⁻¹; [α]_D: +21° (c 1.0,
488 CH₂Cl₂).

489 **Boc-L-Phe-OAll (6).** Boc-L-Phe-OH **5** (799 mg, 3.0 mmol) was
490 dissolved in DMF (10 mL) and cooled to 0 °C in an ice bath. ⁱPr₂NEt
491 (1.57 mL, 9 mmol) was added dropwise, followed by allyl bromide
492 (280 μL, 3.3 mmol). The solution was allowed to warm to rt and
493 stirred for 16 h. The reaction mixture was diluted with EtOAc (40
494 mL), and then washed with water (2 × 30 mL) and brine (30 mL).
495 The organic phase was dried with anhydrous MgSO₄, concentrated in
496 vacuo, and purified via flash column chromatography to afford allyl
497 ester **6** as a yellow oil (905 mg, 99% yield). ¹H NMR (CDCl₃, 400
498 MHz) δ (ppm): 7.33–7.13 (m, 5H), 5.88 (ddt, J = 5.7, 11.0, 16.2 Hz,
499 1H), 5.32 (dq, J = 2.0, 17.3 Hz, 1H), 5.26 (dd, J = 2.0, 10.5 Hz, 1H),
500 4.62 (dt, J = 1.5, 6.0 Hz, 2H), 3.18–3.05 (m, 2H), 1.44 (s, 9H). ¹³C
501 NMR (CDCl₃, 100 MHz) δ (ppm): 171.6, 155.1, 135.9, 131.5, 129.4,
502 128.5, 127.2, 118.9, 79.9, 65.9, 54.5, 38.4, 28.3. These data are in
503 agreement with those previously reported by Lang et al.⁴⁹

504 **L-Phe-OAll (7).** Boc-L-Phe-OAll (**6**) (885 mg, 2.90 mmol) was
505 treated with TFA in CH₂Cl₂ (10 mL, 1:1 v/v). The reaction mixture
506 was stirred at room temperature for 1 h, after which the TFA/CH₂Cl₂
507 solvent mixture was removed under a gentle stream of nitrogen. The
508 reaction mixture was diluted into CH₂Cl₂ (30 mL) and then washed
509 with water (2 × 30 mL) and brine (30 mL). The organic phase was
510 dried with anhydrous MgSO₄ and then concentrated in vacuo to
511 afford **7** as a yellow oil (592 mg, 99% yield). ¹H NMR (CDCl₃, 400

MHz) δ (ppm): 7.27–7.07 (m, 5H), 5.70 (ddt, J = 5.7, 11.0, 16.2 Hz, 512
1H), 5.20–5.16 (m, 2H), 4.49 (d, J = 6.1 Hz, 2H), 4.20 (t, J = 7.0 Hz, 513
1H), 3.24–3.11 (m, 2H); ¹³C NMR (CDCl₃, 100 MHz) δ (ppm): 514
168.6, 132.9, 130.2, 129.3, 128.2, 120.2, 67.4, 54.3, 36.2. These data 515
are in agreement with those previously reported by Lang et al.⁴⁹ 516

Fmoc-L-Asp(OtBu)-L-Phe-OAll (8). A solution of Fmoc-L-Asp- 517
(OtBu)-OH (1.21 g, 2.91 mmol), HATU (1.11 mg, 2.90 mmol), and 518
N-methylmorpholine (NMM, 1 mL, 9.0 mmol) in DMF (final amino 519
acid concentration 0.1 M) was added to a reaction vessel containing 520
H-L-Phe-OAll **7** (533 mg, 2.6 mmol). The reaction was stirred for 2 h, 521
after which the solvent was removed under a stream of nitrogen. The 522
residue was dissolved into CH₂Cl₂ (30 mL), washed with water (2 × 523
30 mL), 2 M HCl (20 mL), saturated aqueous NaHCO₃ solution (20 524
mL), and brine (30 mL). The organic phase was dried with anhydrous 525
MgSO₄, concentrated in vacuo, and purified by flash column 526
chromatography to afford the target compound **S3** as a yellow oil 527
(1.14 g, 74% yield); R_f = 0.40 (EtOAc/hexane, 3:7 v/v). ¹H NMR 528
(CDCl₃, 300 MHz) δ (ppm): 7.72 (d, J = 7.9 Hz, 2H), 7.53 (d, J = 529
7.5 Hz, 2H), 7.36 (dd, J = 7.1, 7.4 Hz, 2H), 7.30–6.96 (m, 7H), 5.90 530
(d, J = 7.6 Hz, 1H), 5.79 (ddt, J = 6.0, 11.2, 16 Hz, 1H), 5.22 (dd, J = 531
18, 10.6 Hz, 2H), 4.80 (dd, J = 13.1, 6.2 Hz, 1H), 4.50 (m, 1H), 532
4.37–4.27 (m, 2H), 4.17 (dd, J = 14.1, 7.1 Hz, 1H), 3.07 (dd, J = 6.2, 533
5.7 Hz, 2H), 2.84 (dd, 17, 4.0 Hz, 1H), 2.56 (dd, 17, 6.6 Hz, 1H), 534
1.40 (s, 9H); ¹³C NMR (CDCl₃, 75 MHz) δ (ppm): 171.2, 170.6, 535
170.2, 155.9, 143.7, 141.3, 135.6, 131.4, 129.3, 128.5, 127.7, 127.1, 536
125.1, 120.0, 119.0, 81.9, 67.3, 66.0, 53.6, 50.9, 47.0, 37.8, 28.5; 537
HRMS: (+ESI) Calc. for 598.2679 [M + Na]⁺, found: 598.2681 [M + 538
Na]⁺; IR (ATR): ν_{max} = 3301, 3066, 3030, 2924, 2854, 1711, 1661, 539
1532, 1449, 1248, 1211, 1050, 738, 701 cm⁻¹; [α]_D: +6.25° (c 1.0, 540
CH₂Cl₂). 541

In Vitro Assessment of Vaccine Adjuvant Activity. Human 542
Embryonic Kidney 293 (HEK293; ATCC CRL-1573) cells, stably 543
transfected with a plasmid expressing YFP-TLR2 fusion protein⁵⁰ that 544
secretes IL-8 upon TLR activation (kindly provided by A/Prof Ashley 545
Mansell, Monash University), were used as a reporter of TLR2 546
stimulation by Pam₂Cys in the vaccine construct. Cells were grown in 547
Dulbecco's modified Eagle's medium (Gibco, MA) with D-glucose 548
(4.5 g/L), L-glutamine (3.996 mM), penicillin–streptomycin (100 U/ 549
mL; Gibco), geneticin (0.5 mg/mL; Gibco), and 10% heat-inactivated 550
fetal calf serum (FCS) at 37 °C and 5% CO₂. After seeding 2 × 10⁵ 551
cells/well of a 96-well flat-bottom plate (Corning) and allowing cells 552
to adhere, the cells were stimulated in triplicate for 16–18 h with 553
vaccine candidate **1** (33.5 μg/mL; such that Pam₂Cys-SKKKK- 554
triethyleneglycolate was at 10 μg/mL, the optimal concentration for 555
stimulation of this cell line as determined by previous experiments, 556
ESAT6_{1–20} ~15 μg/mL and TB10.4_{3–11} ~8 μg/mL). As a 557
comparison, Pam₂Cys-SKKKK-triethyleneglycolate (10 μg/mL), 558
ESAT6_{1–20} peptide (15 μg/mL), or TB10.4_{3–11} peptide (Genscript; 559
8 μg/mL) was also used as a stimulus. Supernatants were collected 560
and IL-8 secretion determined as a measure of stimulation of TLR2 561
by ELISA (Biolegend), according to manufacturer's instructions. Data 562
shown are representative of two independent experiments. 563

Mice and Immunization Procedures. All murine experiments 564
were conducted with the approval of the Sydney Local Health District 565
Animal Welfare Committee (protocol numbers 2013/054, 2013/075, 566
and 2016/044), in full compliance with local and institutional 567
guidelines. Female C57BL/6 6- to 8-week old mice were obtained 568
from Animal BioResources (Moss Vale, NSW, Australia). The mice 569
were housed in the Centenary Institute animal facility under SPF 570
conditions. For i.n. administration, mice were anesthetized by 571
intraperitoneal injection of ketamine/xylazine solution (50 mg/6.25 572
mg/kg). Vaccine (14.2 μg, equivalent to 10 μg peptide) in phosphate- 573
buffered saline (PBS; 50 μL final volume, such that the vaccine 574
reached the deep lung) was applied to the nares and mice allowed to 575
inhale the solution. Mice receiving subcutaneous vaccines (14.2 μg for 576
protection studies and 56.8 μg for immunogenicity studies, equivalent 577
to 10 or 40 μg peptide respectively; in PBS, 200 μL final volume) 578
were anesthetized with gaseous isoflurane (4%) and injected at the 579
base of tail. No adverse effects were observed in mice receiving this 580
vaccine by either mucosal or subcutaneous routes. Mice received 3 581

582 vaccinations 2 weeks apart and proceeded to either immunogenicity
583 study at 3 weeks after last vaccination, or Mtb challenge at 6 weeks
584 after last vaccination. Mice receiving BCG were vaccinated s.c. once
585 only with 5×10^5 CFU, 10 weeks prior to Mtb challenge.

586 **Bacterial Strains and Growth Conditions.** *Mangora bovis* BCG
587 Pasteur 1173P2 and Mtb H37Rv (BEI Resources, NIAID, NIH, NR-
588 13648) were cultured at 37 °C in Middlebrook 7H9 (Difco) broth
589 supplemented with albumin-dextrose-catalase (ADC; 10% v/v),
590 Tween-80 (0.05% v/v), and glycerol (0.2% v/v). To enumerate,
591 cultures were plated onto Middlebrook 7H10 or 7H11 (Difco) agar,
592 supplemented with oleic-acid-albumin-dextrose catalase (10% v/v)
593 and glycerol (0.5% v/v) and incubated at 37 °C for up to 21 days.

594 **Experimental Mtb Infection.** At 6 weeks after 3 immunizations,
595 mice received a low-dose aerosol infection (100 CFU) in an
596 inhalation exposure system (Glas-Col, Terre Haute, IN). At 4
597 weeks after challenge, serial dilutions of lung and spleen homogenates
598 were plated to enumerate the bacterial loads.

599 **Collection and Processing of Murine Organs for Leukocyte
600 Isolation.** Mice were sacrificed via CO₂ asphyxiation, the tissues
601 removed aseptically and maintained at 4 °C. Circulating blood was
602 removed from the lung lobes by perfusion with an injection of PBS
603 and heparin (20 U/mL; Sigma) into the right atrium of the heart. For
604 isolation of leukocytes, diced tissue was digested with collagenase type
605 4197 (50 U/mL; Sigma) and DNase I (13 µg/mL; Sigma) at 37 °C
606 for 45 min, followed by homogenization and multiple filtration steps
607 through a 70 µm sieve. The spleen, mediastinal lymph node (MLN)
608 of i.n. immunized mice or inguinal lymph nodes (ILN) of s.c.
609 immunized mice was homogenized through a 70 µm sieve and the
610 leukocytes pelleted by centrifugation. Erythrocytes were removed by
611 ACK lysis buffer, then viable leukocytes enumerated by hemocy-
612 tometer or using a BD Countess, with Trypan Blue (0.04%) exclusion.

613 **Polyfunctional T-Lymphocyte Responses to Immunization.**
614 Epitope-specific cytokine production by T-lymphocytes was num-
615 erated by antigen-recall, intracellular immunostaining, and flow
616 cytometry. Single-cell suspensions of up to 4×10^6 lymphocytes
617 were stimulated for 1–2 h (37 °C, 5% CO₂) with ESAT_{6,1–20} or
618 TB10.4_{3–11} peptides (10 µg/mL; Genscript), or with antimouse CD3
619 (1452C11, 5 µg/mL) and antimouse CD28 (37.51, 5 µg/mL; BD
620 Pharmingen) or media alone as controls. Brefeldin A (10 µg/mL;
621 Sigma) was added and further incubation (16 h, 37 °C, 5% CO₂)
622 allowed intracellular accumulation of cytokine. After washing with
623 FACS wash (PBS with 2% FCS), Fc receptors were blocked with
624 antimouse CD16/CD32 (2.4G2; BD Biosciences). Surface markers
625 were labeled with an antimouse CD8-APCCy7 (53-6.7; BD
626 Pharmingen, San Jose, CA), CD4-PECy7 (RM4-5; BD Pharmingen),
627 CD3-PerCPCy5.5 (17A2; Biolegend, San Diego, CA), and Live/Dead
628 fixable blue dead cell stain (Invitrogen, CA) in FACS wash, then the
629 cells were washed thoroughly. Cells were fixed using BD Cytofix/
630 perm, followed by thorough washing with BD Perm/Wash. To label
631 intracellular cytokines, cells were incubated with antimouse IFNγ-
632 FITC (XMG1.2; BD Pharmingen), IL-17A-PB (TC11-18H10.1;
633 Biolegend), TNFα-PE/APC (MP6-XT22; Biolegend), and IL-2-
634 APC/PE (JES6-SH4; Biolegend) prepared in BD Perm/Wash buffer
635 and then washed. Compensation controls were prepared by
636 immunostaining BD CompBeads with the same antibody utilized in
637 the experimental panel, except for live dead staining, in which case
638 murine leukocytes were labeled in the same manner as experimental
639 samples. Immunostained cells or beads were fixed in 10% neutral
640 buffered formalin prior to the acquisition of the data using an
641 LSRFortessa or LSRII SL flow analyser (BD Biosciences) and analysis
642 using FlowJo (Tree Star Inc.).

643 **Statistical Analysis.** Statistical analysis was performed using
644 GraphPad Prism 6 or 7 software (GraphPad Software, La Jolla, CA),
645 as detailed in figure legends. Differences between two groups were
646 analyzed by Students *t*-test, or between multiple groups by one- or
647 two-way analysis of variance (ANOVA) with Tukey's or Dunnett's
648 multiple comparisons test and were considered significant when *p*
649 values were ≤ 0.05 (**p* < 0.05, ***p* < 0.01, ****p* < 0.001, *****p* <
650 0.0001).

■ ASSOCIATED CONTENT

651

📄 Supporting Information

652

The Supporting Information is available free of charge on the
ACS Publications website at DOI: 10.1021/acs.jmed-
chem.9b00832.

653

654

655

NMR spectra, MALDI-TOF mass spectrum of **1**, and
immunological data (PDF)

656

657

Molecular formula strings (CSV)

658

■ AUTHOR INFORMATION

659

Corresponding Authors

660

*E-mail: w.britton@centenary.org.au (W.J.B.).

661

*E-mail: richard.payne@sydney.edu.au (R.J.P.).

662

ORCID

663

Richard J. Payne: 0000-0002-3618-9226

664

Author Contributions

665

||A.S.A. and D.M.M. contributed equally to this work.

666

Author Contributions

667

All authors have given approval to the final version of the
manuscript.

668

669

Funding

670

This work was supported by the National and Medical
Research Council of Australia Project Grant (APP1044343),
Centre for Research Excellence in Tuberculosis Control
(APP1043225), and the NSW Government through its
infrastructure grant to the Centenary Institute. A.S.A.,
D.M.M., and C.C.H. each received an Australian Postgraduate
Award.

671

672

673

674

675

676

677

Notes

678

The authors declare no competing financial interest.

679

■ ACKNOWLEDGMENTS

680

We thank Prof J Triccas, the University of Sydney, for
provision of BCG stocks, Dr B Saunders, the University of
Technology Sydney, for provision of antimouse CD3 antibody
and A/Prof A Mansell, Monash University, for provision of
HEK-TLR2 reporter cell line stocks. We thank Dr G
Nagalingam, Dr D Quan, Dr L Lin, Dr M Flórido, and Dr S
Rudrawar, the Centenary Institute Animal Facility and Sydney
Cytometry, for technical assistance and advice.

681

682

683

684

685

686

687

688

■ ABBREVIATIONS

689

BCG, *Mycobacterium bovis* bacille Calmette–Guérin; DIC,
N,N'-diisopropylcarbodiimide; i.n., intranasal; Mtb, *Mycobac-
terium tuberculosis*; Oxyma, ethyl (hydroxyimino)cianoacetate;
PyBOP, (benzotriazole-1-yloxy)tripyrrolidinophosphonium
hexafluorophosphate; SPPS, solid-phase peptide synthesis;
TCEP, tris(2-carboxyethyl)phosphine hydrochloride; TFET,
2,2,2-trifluoroethanethiol; Th, T-helper; VA-044, 2,2'-azobis-
[2-(2-imidazolin-2-yl)propane]dihydrochloride

690

691

692

693

694

695

696

697

■ REFERENCES

698

- (1) Kaufmann, S. H. E.; Hussey, G.; Lambert, P.-H. New vaccines
for tuberculosis. *Lancet* **2010**, *375*, 2110–2119. 700
- (2) *Global Tuberculosis Report*; World Health Organization: Geneva,
2018. 701
- (3) Andersen, P.; Doherty, T. M. The success and failure of BCG-
implications for a novel tuberculosis vaccine. *Nat. Rev. Microbiol.*
2005, *3*, 656–662. 702
- (4) Marais, B. J.; Sintchenko, V. Epidemic spread of multidrug-
resistant tuberculosis in China. *Lancet Infect. Dis.* **2017**, *17*, 238–239. 703

- 708 (5) Marais, B. J.; Mlambo, C. K.; Rastogi, N.; Zozio, T.; Duse, A. G.;
709 Victor, T. C.; Marais, E.; Warren, R. M. Epidemic spread of
710 multidrug-resistant tuberculosis in Johannesburg, South Africa. *J. Clin.*
711 *Microbiol.* **2013**, *51*, 1818–1825.
- 712 (6) Ragonnet, R.; Trauer, J. M.; Denholm, J. T.; Marais, B. J.;
713 McBryde, E. S. High rates of multidrug-resistant and rifampicin-
714 resistant tuberculosis among re-treatment cases: where do they come
715 from? *BMC Infect. Dis.* **2017**, *17*, No. 36.
- 716 (7) Nemes, E.; Geldenhuys, H.; Rozot, V.; Rutkowski, K. T.;
717 Ratangee, F.; Bilek, N.; Mabwe, S.; Makhethhe, L.; Erasmus, M.; Toefy,
718 A.; Mulenga, H.; Hanekom, W. A.; Self, S. G.; Bekker, L.-G.; Ryall, R.;
719 Gurunathan, S.; DiazGranados, C. A.; Andersen, P.; Kromann, I.;
720 Evans, T.; Ellis, R. D.; Landry, B.; Hokey, D. A.; Hopkins, R.;
721 Ginsberg, A. M.; Scriba, T. J.; Hatherill, M. Prevention of *M.*
722 *tuberculosis* infection with H4:IC31 vaccine or BCG revaccination. *N.*
723 *Engl. J. Med.* **2018**, *379*, 138–149.
- 724 (8) Van Der Meeren, O.; Hatherill, M.; Nduba, V.; Wilkinson, R. J.;
725 Muyoyeta, M.; Van Brakel, E.; Ayles, H. M.; Henostroza, G.;
726 Thienemann, F.; Scriba, T. J.; Diacon, A.; Blatner, G. L.; Demoitié,
727 M.-A.; Tameris, M.; Malahleha, M.; Innes, J. C.; Hellström, E.;
728 Martinson, N.; Singh, T.; Akite, E. J.; Khatoon Azam, A.; Bollaerts, A.;
729 Ginsberg, A. M.; Evans, T. G.; Gillard, P.; Tait, D. R. Phase 2b
730 controlled trial of M72/AS01E vaccine to prevent tuberculosis. *N.*
731 *Engl. J. Med.* **2018**, *379*, 1621–1634.
- 732 (9) Sabin, A. B. Immunization against measles by aerosol. *Rev. Infect.*
733 *Dis.* **1983**, *5*, 514–523.
- 734 (10) Saluja, V.; Amorij, J. P.; Kapteyn, J. C.; de Boer, A. H.; Frijlink,
735 H. W.; Hinrichs, W. L. J. A comparison between spray drying and
736 spray freeze drying to produce an influenza subunit vaccine powder
737 for inhalation. *J. Controlled Release* **2010**, *144*, 127–133.
- 738 (11) Cutts, F. T.; Clements, C. J.; Bennett, J. V. Alternative routes of
739 measles immunization: a review. *Biologicals* **1997**, *25*, 323–338.
- 740 (12) Lu, D.; Hickey, A. J. Pulmonary vaccine delivery. *Expert Rev.*
741 *Vaccines* **2007**, *6*, 213–216.
- 742 (13) Perdomo, C.; Zedler, U.; Kühl, A. A.; Lozza, L.; Saikali, P.;
743 Sander, L. E.; Vogelzang, A.; Kaufmann, S. H. E.; Kupz, A. Mucosal
744 BCG vaccination induces protective lung-resident memory T cell
745 populations against tuberculosis. *mBio* **2016**, *7*, No. e01686-16.
- 746 (14) Tameris, M. D.; Hatherill, M.; Landry, B. S.; Scriba, T. J.;
747 Snowden, M. A.; Lockhart, S.; Shea, J. E.; McClain, J. B.; Hussey, G.
748 D.; Hanekom, W. A.; Mahomed, H.; McShane, H. Safety and efficacy
749 of MVA85A, a new tuberculosis vaccine, in infants previously
750 vaccinated with BCG: a randomised, placebo-controlled phase 2b
751 trial. *Lancet* **2013**, *1*, 60177–60174.
- 752 (15) Satti, I.; Meyer, J.; Harris, S. A.; Thomas, Z.-R. M.; Griffiths, K.;
753 Antrobus, R. D.; Rowland, R.; Ramon, R. L.; Smith, M.; Sheehan, S.;
754 Bettinson, H.; McShane, H. Safety and immunogenicity of a candidate
755 tuberculosis vaccine MVA85A delivered by aerosol in BCG-
756 vaccinated healthy adults: a phase 1, double-blind, randomised
757 controlled trial. *Lancet Infect. Dis.* **2014**, *14*, 939–946.
- 758 (16) White, A. D.; Sibley, L.; Dennis, M. J.; Gooch, K.; Betts, G.;
759 Edwards, N.; Reyes-Sandoval, A.; Carroll, M. W.; Williams, A.; Marsh,
760 P. D.; McShane, H.; Sharpe, S. A. Evaluation of the safety and
761 immunogenicity of a candidate tuberculosis vaccine, MVA85A,
762 delivered by aerosol to the lungs of macaques. *Clin. Vaccine Immunol.*
763 **2013**, *20*, 663–672.
- 764 (17) Kaufmann, S. H. E. Future vaccination strategies against
765 tuberculosis: thinking outside the box. *Immunity* **2010**, *33*, 567–577.
- 766 (18) Parida, S. K.; Kaufmann, S. H. E. Novel tuberculosis vaccines
767 on the horizon. *Curr. Opin. Immunol.* **2010**, *22*, 374–384.
- 768 (19) Ingale, S.; Wolfert, M. A.; Gaekwad, J.; Buskas, T.; Boons, G. J.
769 Robust immune responses elicited by a fully synthetic three-
770 component vaccine. *Nat. Chem. Biol.* **2007**, *3*, 663–667.
- 771 (20) McDonald, D. M.; Wilkinson, B. L.; Corcilius, L.; Thaysen-
772 Andersen, M.; Byrne, S. N.; Payne, R. J. Synthesis and immunological
773 evaluation of self-adjuncting MUC1-macrophage activating lip-
774 opeptide 2 conjugate vaccine candidates. *Chem. Commun.* **2014**, *50*,
775 10273–10276.
- (21) Moyle, P. M.; Olive, C.; Good, M. F.; Toth, I. Method for the
synthesis of highly pure vaccines using the lipid core peptide system. *J.*
Pept. Sci. **2006**, *12*, 800–807.
- (22) Wilkinson, B. L.; Day, S.; Malins, L. R.; Apostolopoulos, V.;
Payne, R. J. Self-adjuncting multicomponent cancer vaccine
candidates combining per-glycosylated MUC1 glycopeptides and
the Toll-like receptor 2 agonist Pam₃CysSer. *Angew. Chem., Int. Ed.*
2011, *50*, 1635–1639.
- (23) Cai, H.; Chen, M.-S.; Sun, Z.-Y.; Zhao, Y.-F.; Kunz, H.; Li, Y.-
M. Self-adjuncting synthetic antitumor vaccines from MUC1
glycopeptides conjugated to T-cell epitopes from tetanus toxoid.
Angew. Chem., Int. Ed. **2013**, *52*, 6106–6110.
- (24) Wilkinson, B. L.; Day, S.; Chapman, R.; Perrier, S.;
Apostolopoulos, V.; Payne, R. J. Synthesis and immunological
evaluation of self-assembling and self-adjuncting tricomponent
glycopeptide cancer-vaccine candidates. *Chem. - Eur. J.* **2012**, *18*,
16540–16548.
- (25) Zom, G. G.; Welters, M. J.; Loof, N. M.; Goedemans, R.;
Lougheed, S.; Valentijn, R. R.; Zandvliet, M. L.; Meeuwenoord, N. J.;
Melief, C. J.; de Gruijl, T. D.; Van der Marel, G. A.; Filippov, D. V.;
Ossendorp, F.; Van der Burg, S. H. TLR2 ligand-synthetic long
peptide conjugates effectively stimulate tumor-draining lymph node T
cells of cervical cancer patients. *Oncotarget* **2016**, *7*, 67087–67100.
- (26) Xu, Z.; Moyle, P. M. Bioconjugation approaches to producing
subunit vaccines composed of protein or peptide antigens and
covalently attached Toll-like receptor ligands. *Bioconjugate Chem.*
2018, *29*, 572–586.
- (27) Tyne, A. S.; Chan, J. G.; Shanahan, E. R.; Atmosukarto, I.;
Chan, H. K.; Britton, W. J.; West, N. P. TLR2-targeted secreted
proteins from *Mycobacterium tuberculosis* are protective as powdered
pulmonary vaccines. *Vaccine* **2013**, *31*, 4322–4329.
- (28) Andersson, M.; Lutay, N.; Hallgren, O.; Westergren-Thorsson,
G.; Svensson, M.; Godaly, G. *Mycobacterium bovis* bacilli Calmette-
Guerin regulates leukocyte recruitment by modulating alveolar
inflammatory responses. *Innate Immun.* **2012**, *18*, 531–540.
- (29) Hertz, C. J.; Wu, Q.; Porter, E. M.; Zhang, Y. J.; Weismüller, K.-
H.; Godowski, P. J.; Ganz, T.; Randell, S. H.; Modlin, R. L. Activation
of Toll-like receptor 2 on human tracheobronchial epithelial cells
induces the antimicrobial peptide human β defensin-2. *J. Immunol.*
2003, *171*, 6820–6826.
- (30) Li, Y.; Wang, Y.; Liu, X. The role of airway epithelial cells in
response to *Mycobacteria* infection. *Clin. Dev. Immunol.* **2012**,
No. 791392.
- (31) Gupta, N.; VEDI, S.; Kunimoto, D. Y.; Agrawal, B.; Kumar, R.
Novel lipopeptides of ESAT-6 induce strong protective immunity
against *Mycobacterium tuberculosis*: Routes of immunization and TLR
agonists critically impact vaccine's efficacy. *Vaccine* **2016**, *34*, 5677–
5688.
- (32) Dawson, P. E.; Muir, T. W.; Clark-Lewis, I.; Kent, S. B.
Synthesis of proteins by native chemical ligation. *Science* **1994**, *266*,
776–779.
- (33) Thompson, R. E.; Liu, X.; Alonso-García, N.; Pereira, P. J. B.;
Jolliffe, K. A.; Payne, R. J. Trifluoroethanethiol: an additive for
efficient one-pot peptide ligation–desulfurization chemistry. *J. Am.*
Chem. Soc. **2014**, *136*, 8161–8164.
- (34) Hanna, C. C.; Kulkarni, S. S.; Watson, E. E.; Premjee, B.;
Payne, R. J. Solid-phase synthesis of peptide selenoesters via a side-
chain anchoring strategy. *Chem. Commun.* **2017**, *53*, 5424–5427.
- (35) Wang, P.; Miranda, L. P. Fmoc-protein synthesis: preparation
of peptide thioesters using a side-chain anchoring strategy. *Int. J. Pept.*
Res. Ther. **2005**, *11*, 117–123.
- (36) Ficht, S.; Payne, R. J.; Guy, R. T.; Wong, C. H. Solid-phase
synthesis of peptide and glycopeptide thioesters through side-chain-
anchoring strategies. *Chem. Eur. J.* **2008**, *14*, 3620–3629.
- (37) Saunders, B. M.; Britton, W. J. Life and death in the granuloma:
immunopathology of tuberculosis. *Immunol. Cell Biol.* **2007**, *85*, 103–
111.

- 843 (38) Zygmunt, B. M.; Rharbaoui, F.; Groebe, L.; Guzman, C. A.
844 Intranasal immunization promotes Th17 immune responses. *J.*
845 *Immunol.* **2009**, *183*, 6933–6938.
- 846 (39) Orr, M. T.; Beebe, E. A.; E. Hudson, T.; Argilla, D.; Huang, P.-
847 W. D.; Reese, V. A.; Fox, C. B.; Reed, S. G.; Coler, R. N. Mucosal
848 delivery switches the response to an adjuvanted tuberculosis vaccine
849 from systemic Th1 to tissue-resident Th17 responses without
850 impacting the protective efficacy. *Vaccine* **2015**, *33*, 6570–6578.
- 851 (40) Ouyang, W.; Kolls, J. K.; Zheng, Y. The biological functions of
852 T helper 17 cell effector cytokines in inflammation. *Immunity* **2008**,
853 *28*, 454–467.
- 854 (41) Okamoto Yoshida, Y.; Umemura, M.; Yahagi, A.; O'Brien, R.
855 L.; Ikuta, K.; Kishihara, K.; Hara, H.; Nakae, S.; Iwakura, Y.;
856 Matsuzaki, G. Essential role of IL-17A in the formation of a
857 Mycobacterial infection-induced granuloma in the lung. *J. Immunol.*
858 **2010**, *184*, 4414–4422.
- 859 (42) Khader, S. A.; Bell, G. K.; Pearl, J. E.; Fountain, J. J.; Rangel-
860 Moreno, J.; Cilley, G. E.; Shen, F.; Eaton, S. M.; Gaffen, S. L.; Swain,
861 S. L.; Locksley, R. M.; Haynes, L.; Randall, T. D.; Cooper, A. M. IL-
862 23 and IL-17 in the establishment of protective pulmonary CD4+ T
863 cell responses after vaccination and during *Mycobacterium tuberculosis*
864 challenge. *Nat. Immunol.* **2007**, *8*, 369–377.
- 865 (43) Noack, M.; Miossec, P. Th17 and regulatory T cell balance in
866 autoimmune and inflammatory diseases. *Autoimmun. Rev.* **2014**, *13*,
867 668–677.
- 868 (44) Cooper, A. M. Editorial: Be careful what you ask for: is the
869 presence of IL-17 indicative of immunity? *J. Leukocyte Biol.* **2010**, *88*,
870 221–223.
- 871 (45) Uranga, S.; Marinova, D.; Martin, C.; Aguilo, N. Protective
872 efficacy and pulmonary immune response following subcutaneous and
873 intranasal BCG administration in mice. *J. Vis. Exp.* **2016**, *115*,
874 No. e54440.
- 875 (46) Lindenstrøm, T.; Woodworth, J.; Dietrich, J.; Aagaard, C.;
876 Andersen, P.; Agger, E. M. Vaccine-induced Th17 cells are maintained
877 long-term postvaccination as a distinct and phenotypically stable
878 memory subset. *Infect. Immun.* **2012**, *80*, 3533–3544.
- 879 (47) Wozniak, T. M.; Saunders, B. M.; Ryan, A. A.; Britton, W. J.
880 *Mycobacterium bovis* BCG-specific Th17 cells confer partial protection
881 against *Mycobacterium tuberculosis* infection in the absence of gamma
882 interferon. *Infect. Immun.* **2010**, *78*, 4187–4194.
- 883 (48) McShane, H.; Williams, A. A review of preclinical animal
884 models utilised for TB vaccine evaluation in the context of recent
885 human efficacy data. *Tuberculosis* **2014**, *94*, 105–110.
- 886 (49) Lang, S. B.; O'Nele, K. M.; Douglas, J. T.; Tunge, J. A. Dual
887 catalytic decarboxylative allylations of alpha-amino acids and their
888 divergent mechanisms. *Chem. - Eur. J.* **2015**, *21*, 18589–18593.
- 889 (50) Latz, E.; Visintin, A.; Lien, E.; Fitzgerald, K. A.; Monks, B. G.;
890 Kurt-Jones, E. A.; Golenbock, D. T.; Espevik, T. Lipopolysaccharide
891 rapidly traffics to and from the golgi apparatus with the Toll-like
892 receptor 4-MD-2-CD14 complex in a process that is distinct from the
893 initiation of signal transduction. *J. Biol. Chem.* **2002**, *277*, 47834–
894 47843.